DOI: 10.1002/chem.201000205

Redox-Tuning Endohedral Fullerene Spin States: From the Dication to the Trianion Radical of $Sc_3N@C_{80}(CF_3)_2$ in Five Reversible Single-Electron Steps

Alexey A. Popov,*[a] Natalia B. Shustova,[b] Anna L. Svitova,[a] Mary A. Mackey,[c] Curtis E. Coumbe,[c] J. Paige Phillips,*[c] Steven Stevenson,*[c] Steven H. Strauss,*[b] Olga V. Boltalina,*[b] and Lothar Dunsch*[a]

Synthetic/separation procedures for endohedral fullerenes, especially nitride cluster fullerenes $M_3N@C_{2n}$ (NCFs), have progressed to the point in which sufficient amounts are now available for the exploration of their electronic and chemical properties.[1] NCFs were recently found to be superior to C_{60} in stabilizing charge-separated states in donor–acceptor dyads.[2] In contrast to the wealth of information about oxidized (cationic) and reduced (anionic) C_{60} derivatives, much less is known about NCF cations and anions, and even less is known about their derivatives. NCFs exhibit electrochemically irreversible reductions, at slow scan rates, that are chemically reversible.[1e,f] On the other hand, some $M_3N@C_{80}(X)_n$ derivatives have reversible electron-transfer steps even at low scan rates[2] (hereinafter C_{80} shall specifically denote the C_{80}-I_h(7) cage). Spectroscopic data for NCF ions are limited to 1) ex situ ESR spectra of $Sc_3N@C_{80}^{-}$[3] and the monoanion of a pyrrolidino cycloadduct of $Y_3N@C_{80}$[4] and 2) in situ ESR/Vis/NIR spectra of $Sc_3N@C_{68}^{+}$ and $Sc_3N@C_{68}^{-}$.[5]

The trifluoromethylation of NCFs was recently developed and several $Sc_3N@C_{80}(CF_3)_n$ derivatives were isolated and characterized by mass spectrometry, UV/Vis and NMR spectroscopy, and single-crystal X-ray diffraction.[6] We now report the existence of the mono- and dications and the mono-, di-, and trianions of the simplest derivative, $Sc_3N@C_{80}(CF_3)_2$ (I), and an in-depth study of three of them by ESR and Vis/NIR spectroelectrochemistry. The cyclic voltammetry of I, shown in Figure 1, exhibits three reversible one-electron reductions at −1.16, −1.65, and −2.04 V versus $Fe(Cp)_2^{+/0}$ and two reversible one-electron oxidations at 0.47 and 0.60 V versus $Fe(Cp)_2^{+/0}$. The dotted lines show that I has a smaller +/− electrochemical gap than $Sc_3N@C_{80}$ (II); the 0/− and +/0 $E_{1/2}$ values for I are shifted, respec-

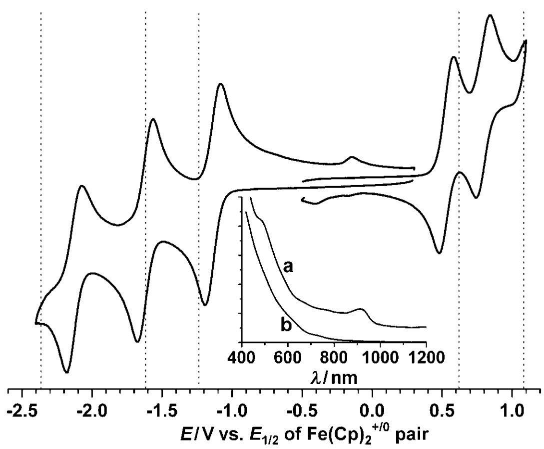

Figure 1. Cyclic voltammetry of $Sc_3N@C_{80}(CF_3)_2$ (1,2-$C_6H_4Cl_2$ (0.1 M), $TBABF_4$, 25 °C, 20 mV s^{-1}). The dotted lines show the $E_{1/2}$ values of $Sc_3N@C_{80}$ at fast scan rates.[3b,7] The inset shows Vis/NIR absorption spectra of a) $Sc_3N@C_{80}(CF_3)_2$ and b) $Sc_3N@C_{80}$ in toluene.

[a] Dr. A. A. Popov, A. L. Svitova, Prof. Dr. L. Dunsch
Department of Electrochemistry and Conducting Polymers
Leibniz Institute for Solid State and Materials Research
Dresden 01069 (Germany)
Fax: (+49) 351-4659-745
E-mail: a.popov@ifw-dresden.de
l.dunsch@ifw-dresden.de

[b] N. B. Shustova, Prof. S. H. Strauss, Dr. O. V. Boltalina
Department of Chemistry, Colorado State University
Fort Collins, CO 80523 (USA)
Fax: (+1) 970-491-1801
E-mail: olga.boltalina@colostate.edu
steven.strauss@colostate.edu

[c] M. A. Mackey, C. E. Coumbe, Prof. J. P. Phillips, Prof. S. Stevenson
Department of Chemistry and Biochemistry
University of Southern Mississippi, Hattiesburg, MS 39406 (USA)
Fax: (+1) 601-266-6075
E-mail: janice.phillips@usm.edu
steven.stevenson@usm.edu

Supporting information for this article is available on the WWW under http://dx.doi.org/10.1002/chem.201000205.

tively, 0.10 V anodically and 0.15 V cathodically relative to the corresponding $E_{1/2}$ values for II.

The reversibility of the redox processes, even at the low scan rate of 20 $mV\,s^{-1}$, demonstrates that I^{2+}, I^{+}, I^{-}, I^{2-}, and I^{3-} are stable species in 1,2-$C_6H_4Cl_2$ at 25 °C. This enabled us to record and analyze the spectra of the three species with unpaired spin. Figures 2 and 3a show ESR and difference Vis/NIR spectra measured in situ at the first oxidation peak of I. The dependence of the ESR signal on the potential during the voltammetry cycle confirmed the reversible formation of radical cation I^{+} after the first oxidation. Its ESR spectrum consists of a single narrow line (ΔB_{pp} = 0.5 G) with g = 2.0018, accompanied by ^{13}C satellites with $a(^{13}C)$ values of 4.9 and 6.4 G (satellites with $a(^{13}C)$ values smaller than 3 G are also apparent but are not well resolved). The single-line spectrum indicates that there is negligible spin density on the Sc and F atoms in the radical cation I^{+}.

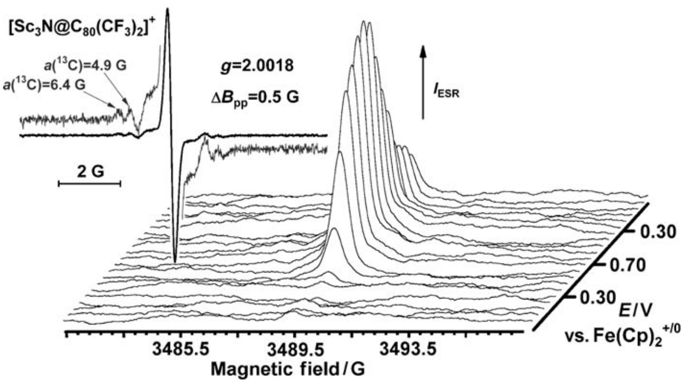

Figure 2. ESR spectrum of the $Sc_3N@C_{80}(CF_3)_2^{+}$ radical cation and the dependence of the integrated ESR spectrum on electrode potential measured in situ during cyclic voltammetry of $Sc_3N@C_{80}(CF_3)_2$ at the first oxidation peak.

The difference Vis/NIR spectra in Figure 3a show that oxidation of I is accompanied by the rise of a broad absorption band at approximately 880 nm (the exact position cannot be determined because of overlap with the negative absorption band at 925 nm due to the consumption of I during the oxidation). Similarly, the radical cation I^{+} exhibits a new band at 620 nm, whereas the negative band at approximately 500 nm corresponds to the disappearance of the 490 nm band of II.

In contrast to I^{+}, and despite the reversible first oxidation of II, we found that II^{+} is ESR-silent. According to DFT calculations, the spin density in II^{+} is localized primarily on the carbon cage,[8] so a narrow ESR signal was expected for this radical cation. In addition, the dependence of the NIR bands for II and II^{+} on potential during the oxidation, which is shown in the Supporting Information, is similar to that observed for the transformation $I \rightarrow I^{+}$ and is also consistent with reversible oxidation. At this point it is not clear why we did not observe an ESR signal for II^{+}. Nevertheless, II^{+} exhibits a strong NIR absorption band at 800 nm, which is blue-shifted relative to the analogous NIR band of I^{+}. A broad band with λ_{max} higher than 1700 nm is also apparent, but is beyond the spectral window of our spectrometer.

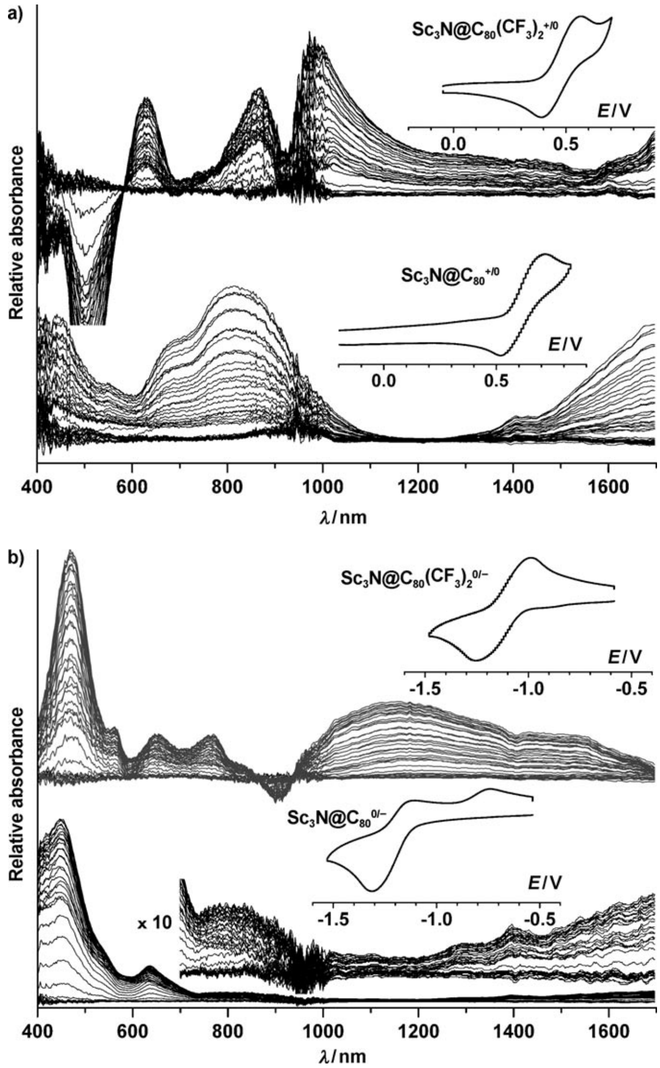

Figure 3. Difference Vis/NIR spectra measured in situ during cyclic voltammetry of $Sc_3N@C_{80}(CF_3)_2$ (top) and $Sc_3N@C_{80}$ (bottom) at a) the first oxidation peak and b) the first reduction peak. Cyclic voltammograms are shown in the insets (scan rate 5 $mV\,s^{-1}$; potentials are versus $Fe(Cp)_2^{+/0}$).

The difference Vis/NIR absorption spectra measured in situ at the first reduction peaks of I and II are shown in Figure 3b. Anion I^{-} exhibits a strong broad NIR band at 1160 nm with a shoulder at 1550 nm as well as additional bands at 645 and 765 nm. Strong absorption is also observed at 470 nm, but its assignment to I^{-} is ambiguous because I also has a strong absorption band in this range. In agreement with previous reports,[3b,7] we found that the first reduction of II is electrochemically irreversible at low voltammetric scan rates. Two reoxidation peaks can be seen in Figure 3b, but only one species was observed in the difference Vis/NIR spectra. Strong absorption-spectra changes for the transformation $II \rightarrow II^{-}$ were only observed in the visible range. A very weak band at 820 nm can be seen in the NIR range in Figure 3b, which was previously assigned to electrochemically or photochemically generated II^-.[2b] However, we did not observe a NIR band at 1000–1100 nm, which was evident in the previously reported spectra.[2b]

The absorption spectra of I^+ and II^+ and of I^- and II^- are sufficiently different such that caution must be used when interpreting the absorption spectra of cationic or anionic derivatives of II (and probably charged derivatives of other NCFs). For example, the transient absorption spectra of charge-transfer states of dyads based on cycloadducts of II should be compared, whenever possible, with monoanionic derivatives of II and not with II^- itself.

A very weak and broad ESR signal attributable to I^- was found during the in situ electrochemical reduction of I. No signal was observed during the in situ reduction of II, but it is known that the ESR spectrum of II^- is very broad,[3] and this apparently precludes its detection in our spectroelectrochemical cell. A stronger ESR spectrum of I^- was obtained by stepping the potential to -1.3 V versus $Fe(Cp)_2^{+/0}$ and accumulating the ESR spectrum during the electrolysis at this potential (see Figure S3 in the Supporting Information). An even better signal-to-noise ratio was achieved when I^- was generated by reacting I with approximately one equivalent of cobaltocene, $Co(Cp)_2$, in 1,2-$C_6H_4Cl_2$. This spectrum is shown in Figure 4a. When II was treated with approximately one equivalent of $Co(Cp)_2$, the ESR spectrum shown in Figure S4 in the Supporting Information, with $a(^{45}Sc) = 55.4$ G and $g = 1.9992$, was in close agreement with the previously reported ESR spectra of II^-.[3]

The ESR spectrum of I^- in Figure 4a was simulated with $g = 1.9958$, three $a(^{45}Sc)$ hyperfine coupling (hfc) constants, 9.34, 9.34, and 10.70 G, and linewidths of 5 G. Therefore, the three Sc atoms in I^- are not equivalent at the ESR timescale, indicating hindered rotation of the Sc_3N cluster. This agrees well with our previous calculations of the energies of the conformers of I.[6a] Hindered rotation of the Y_3N cluster in the monoanion of a pyrrolidino cycloadduct of $Y_3N@C_{80}$ was previously reported by Echegoyen et al.[4] The significant shift of the g value of I^- from the free-electron g_e value of 2.0023 is in harmony with the localization of spin density on the Sc atoms, similar to the situation in II^-. However, the hfc constants for I^- are approximately five times smaller than for II^-, presumably because the unpaired spin density in I^- is distributed on the CF_3 groups and the cage C atoms in their vicinity as well as on the three Sc atoms (see below).

Integration of the ESR spectrum of a solution of I at a potential of -2.10 V versus $Fe(Cp)_2^{+/0}$ resulted in the ESR spectrum shown in Figure 4b, which is assigned to the trianion I^{3-}. This is the first spectroscopic data reported for any endohedral fullerene trianion. The triply reduced species I^{3-} are less stable than the monoanion I^-, and for this reason the spectrum of I^{3-} could only be collected for 30 min (for comparison, the monoanion persisted in solution for at least one day). Nevertheless, the essential features of the ESR spectrum of I^{3-}, which extends over approximately 500 G, are readily apparent. The spectrum was simulated with $g = 2.0006$, $a(^{45}Sc) = 10.8$, 10.8, and 49.2 G, and linewidths of 2.5 G (note that the linewidths are half as large as those in the spectrum of I^-). As in the monoanion I^-, the rotation of the Sc_3N cluster in I^{3-} is slow on the ESR timescale. Furthermore, the large $a(^{45}Sc)$ value of 49.2 G for the unique Sc atom results in significant second-order effects (i.e., the asymmetric nature of the spectrum). Similar second-order effects are also observed in the ESR spectrum of II^-.[3]

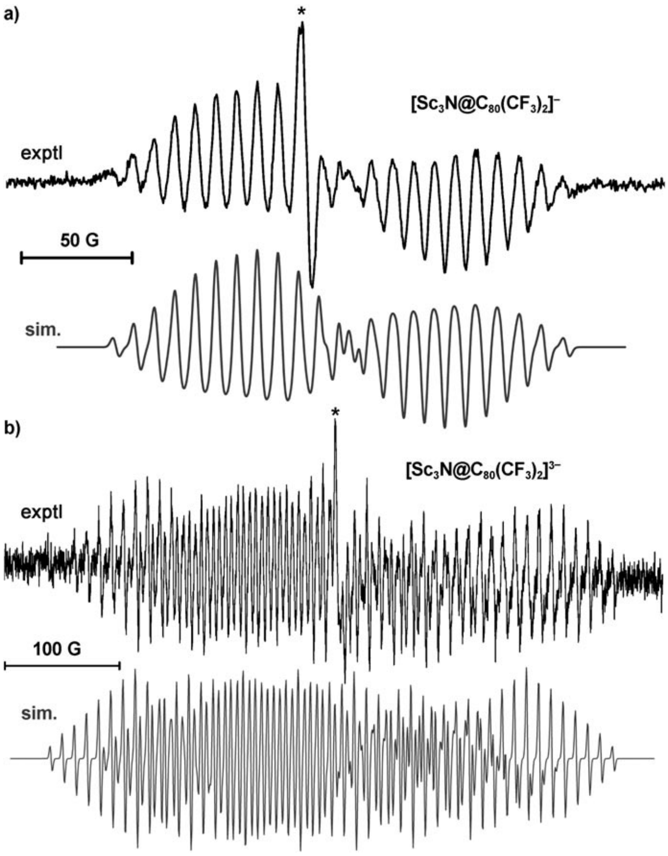

Figure 4. Experimental and simulated ESR spectra of a) $Sc_3N@C_{80}(CF_3)_2^-$ and b) $Sc_3N@C_{80}(CF_3)_2^{3-}$. Simulation parameters: a) $a(^{45}Sc) = 9.34$, 9.34, and 10.70 G, $g = 1.9958$; b) $a(^{45}Sc) = 10.8$, 10.8, and 49.2 G, $g = 2.0006$. The asterisks indicate signals due to an impurity (which contribute less than 1.5% of the total signal). Sim. = simulated.

The DFT-predicted spin-density distributions in the lowest-energy conformers of I^-, I^{3-}, and II^-[8b] are shown in Figure 5. In agreement with the large observed $a(^{45}Sc)$ values, significant spin density is localized on the Sc atoms. Furthermore, the largest amount of spin density in I^{3-} is localized on the unique Sc atom, which is consistent with the 49.2 G hfc constant for this atom (note that the three equal $a(^{45}Sc)$ values in II^- are 55.4 G, which is consistent with the similarly large amounts of spin density on the Sc atoms in that monoanion).

In this work we have determined that there are five accessible and stable charged states of I, demonstrating that the addition of two CF_3 groups to $Sc_3N@C_{80}$ dramatically changes its redox behavior. The NCF derivative I exhibits three reversible reductions and two reversible oxidations.

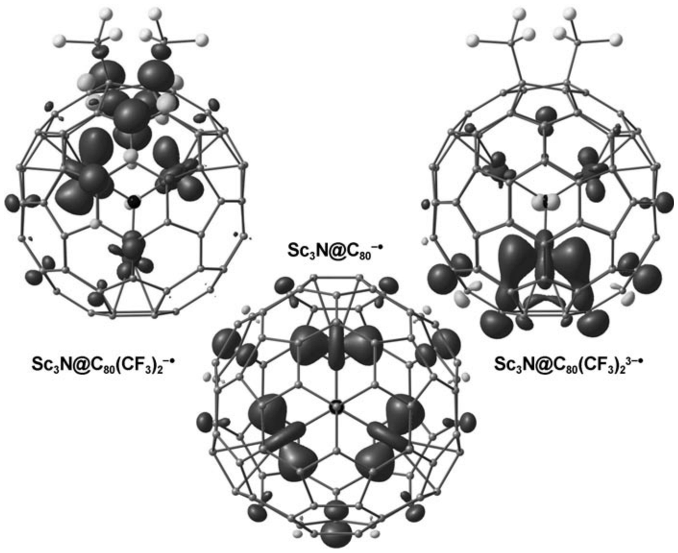

Figure 5. DFT-computed spin-density distribution in the lowest-energy conformers of $Sc_3N@C_{80}(CF_3)_2^-$ (left), $Sc_3N@C_{80}(CF_3)_2^{3-}$ (right), and $Sc_3N@C_{80}^-$ (middle).

We have characterized three of the five charged states, the monocation (I^+), monoanion (I^-), and trianion (I^{3-}) in solution at 25 °C, providing for the first time a broad range of spectroscopically characterized endohedral-fullerene charged states. The spectra indicate a spin-density shift from the fullerene cage to the Sc_3N cluster on going from I^+ to I^{3-}, resulting in a high spin density on one Sc atom in the trianion I^{3-}.

Experimental Section

$Sc_3N@C_{80}(CF_3)_2$ was synthesized as previously described.[6a] Details of the electrochemical and in situ spectroelectrochemical measurements are the same as described in Ref. [9] and can be found in the Supporting Information. Simulation of the ESR spectra was done by using Winsim[10] and SimFonia (Bruker, Germany) software packages. Optimization of the structures was performed at the PBE/TZ2P level by using the PRIRODA code.[11] The spin density was computed at the B3LYP/6–311G*//PBE/TZ2P level by using the Firefly package.[12]

Acknowledgements

This work was supported by the Alexander von Humboldt Foundation (Fellowship to A.A.P.) and U.S. NSF grants (CHE-0707223 to S.H.S. and O.V.B., CHE-0547988 to S.S., CHE-0847481 J.P.P., and GRFP to M.A.M.). The assistance of U. Nitzsche with computational resources in IFW Dresden is gratefully acknowledged.

Keywords: EPR spectroscopy · fullerenes · scandium · spectroelectrochemistry · vibrational spectroscopy

[1] a) S. Stevenson, G. Rice, T. Glass, K. Harich, F. Cromer, M. R. Jordan, J. Craft, E. Hadju, R. Bible, M. M. Olmstead, K. Maitra, A. J. Fisher, A. L. Balch, H. C. Dorn, *Nature* **1999**, *401*, 55–57; b) S. Stevenson, K. Harich, H. Yu, R. R. Stephen, D. Heaps, C. Coumbe, J. P. Phillips, *J. Am. Chem. Soc.* **2006**, *128*, 8829–8835; c) S. Stevenson, M. A. Mackey, M. C. Thompson, H. L. Coumbe, P. K. Madasu, C. E. Coumbe, J. P. Phillips, *Chem. Commun.* **2007**, 4263–4265; d) L. Dunsch, M. Krause, J. Noack, P. Georgi, *J. Phys. Chem. Solids* **2004**, *65*, 309–315; For recent reviews, see: e) L. Dunsch, S. Yang, *Small* **2007**, *3*, 1298–1320; f) M. N. Chaur, F. Melin, A. L. Ortiz, L. Echegoyen, *Angew. Chem.* **2009**, *121*, 7650–7675; *Angew. Chem. Int. Ed.* **2009**, *48*, 7514–7538.

[2] a) J. R. Pinzón, M. E. Plonska-Brzezinska, C. M. Cardona, A. J. Athans, S. S. Gayathri, D. M. Guldi, M. A. Herranz, N. Martin, T. Torres, L. Echegoyen, *Angew. Chem.* **2008**, *120*, 4241–4244; *Angew. Chem. Int. Ed.* **2008**, *47*, 4173–4176; b) J. R. Pinzón, D. C. Gasca, S. G. Sankaranarayanan, G. Bottari, T. Torres, D. M. Guldi, L. Echegoyen, *J. Am. Chem. Soc.* **2009**, *131*, 7727–7734; c) J. R. Pinzón, C. M. Cardona, M. A. Herranz, M. E. Plonska-Brzezinska, A. Palkar, A. J. Athans, N. Martin, A. Rodriguez-Fortea, J. M. Poblet, G. Bottari, T. Torres, S. Shankara Gayathri, D. M. Guldi, L. Echegoyen, *Chem. Eur. J.* **2009**, *15*, 864–877.

[3] a) P. Jakes, K. P. Dinse, *J. Am. Chem. Soc.* **2001**, *123*, 8854–8855; b) B. Elliott, L. Yu, L. Echegoyen, *J. Am. Chem. Soc.* **2005**, *127*, 10885–10888.

[4] L. Echegoyen, C. J. Chancellor, C. M. Cardona, B. Elliott, J. Rivera, M. M. Olmstead, A. L. Balch, *Chem. Commun.* **2006**, 2653–2655.

[5] a) S. F. Yang, P. Rapta, L. Dunsch, *Chem. Commun.* **2007**, 189–191; b) P. Rapta, A. A. Popov, S. F. Yang, L. Dunsch, *J. Phys. Chem. A* **2008**, *112*, 5858–5865.

[6] a) N. B. Shustova, A. A. Popov, M. A. Mackey, C. E. Coumbe, J. P. Phillips, S. Stevenson, S. H. Strauss, O. V. Boltalina, *J. Am. Chem. Soc.* **2007**, *129*, 11676–11677; b) N. B. Shustova, Y.-S. Chen, M. A. Mackey, C. E. Coumbe, J. P. Phillips, S. Stevenson, A. A. Popov, O. V. Boltalina, S. H. Strauss, *J. Am. Chem. Soc.* **2009**, *131*, 17630–17637.

[7] M. Krause, L. Dunsch, *ChemPhysChem* **2004**, *5*, 1445–1449.

[8] a) R. Valencia, A. Rodriguez-Fortea, A. Clotet, C. de Graaf, M. N. Chaur, L. Echegoyen, J. M. Poblet, *Chem. Eur. J.* **2009**, *15*, 10997–11009; b) A. A. Popov, L. Dunsch, *J. Am. Chem. Soc.* **2008**, *130*, 17726–17742.

[9] A. A. Popov, N. B. Shustova, O. V. Boltalina, S. H. Strauss, L. Dunsch, *ChemPhysChem* **2008**, *9*, 431–438.

[10] EPR Spectral Simulation for Microsoft Windows, Public EPR Software Tools, D. A. O'Brien, D. R. Duling, Y. C. Fann, National Institute of Environment Health Sciences, National Institute of Health, **2002**, http://epr.niehs.nih.gov.

[11] a) D. N. Laikov, *Chem. Phys. Lett.* **1997**, *281*, 151–156; b) D. N. Laikov, Y. A. Ustynuk, *Russ. Chem. Bull.* **2005**, *54*, 820–826.

[12] A. A. Granovsky, PC GAMESS/Firefly, version 7.1.C, **2008**, http://classic.chem.msu.su/gran/gamess/index.html.

Received: January 25, 2010
Published online: March 26, 2010

